Soldagem & Inspeção

ISSN 1980-6973 (Online) | ISSN 0104-9224 (Print)
TECHNICAL PAPERS

X-Ray Diffraction Analysis of Residual Stresses in the Premium Rails Welded by Flash Butt Process

Bras Senra de Oliveira[1,2], Lino Alberto Soares Rodrigues[1,3], Ednelson Silva Costa[1,3], Eduardo de Magalhães Braga[1,3], Marcos Allan Leite dos Reis[1,3]

[1] Universidade Federal do Pará – UFPA, Programa de Pós-graduação em Engenharia de Processos – PPGEP, Belém, PA, Brasil.
[2] Instituto de Pesquisas Ecológicas da Amazônia – IPEAM, Belém, PA, Brasil.
[3] Universidade Federal do Pará – UFPA, Faculdade de Engenharia Mecânica – FEM, Laboratório de Caracterização de Materiais Metálicos – LCAM, Belém, PA, Brasil.

How to cite: Oliveira BS, Rodrigues LAS, Costa ES, Braga EM, Reis MAL. X-ray diffraction analysis of residual stresses in the premium rails welded by flash butt process. Soldagem & Inspeção. 2019;25:e2529. https://doi.org/10.1590/0104-9224/SI25.29

Abstract: This work is distinguished by searching for a non-destructive technology, and X-ray diffraction was validated by the XStress 3000 analyser. Measurements of residual stresses in the welded zone of premium pearlitic rails was performed, rail surface hardness of 370 HB and 0.79% carbon content. The welding of the rails was done by flash butt process, performed by Schlatter GAAS 80 stationary equipment. The results of the tensile and compressive stress measurements identified the residual stresses in the welded zone, with specific zones of tensile stresses misplaced at the weld center, with values up to 391 MPa, and compressive stresses, with values up to -166 MPa, as it moves away rails weld center. An important point of this study is the residual stress measurement considering a complete welding process, including: pre-grinding, flash butt welding, heat treatment, finishing grinding and straightening. Lastly, was observed the welding technique potentially can induce residual stresses at rails.

Key-words: X-ray diffraction; Residual stress; Flash butt welding; Pearlitic premium rails; Non-destructive tests.

Análise de Tensões Residuais, Via Difração de Raio-X, em Trilhos Premium Soldados Através do Processo de Centelhamento

Resumo: Este artigo se distingue pela aplicação de um ensaio não destrutivo, onde a difração de raio-x foi validada através do equipamento XStress 3000. Medidas de tensões residuais foram executadas na zona soldada de trilhos perlíticos premium, dureza superficial de 370HB e teor de carbono 0,79%. A soldagem dos trilhos foi executada através do processo de centelhamento elétrico (caldeamento), executado pelo equipamento estacionário Schlatter GAAS 80. Os resultados de tensões residuais identificaram tensões residuais trativas e compressivas na zona soldada, com áreas específicas de tensões trativas deslocadas da região central da solda, com valores de até 391 MPa, e tensões compressivas, com valores de até -166 MPa, conforme as medições iam atingindo a extremidade do corpo de prova. Um ponto importante deste estudo foi a medição de tensões residuais e uma amostra que passou pelo processo completo de soldagem, incluindo: pré-esmerilhamento, soldagem por centelhamento, tratamento térmico, esmerilhamento de acabamento e desempeno. Por fim, foi comprovado que o processo de soldagem pode potencialmente induzir surgimento de tensões residuais nos trilhos.

Palavras-chave: Difração de raio-X; Tensão residual; Soldagem por centelhamento; Trilhos perlíticos premium; Ensaios não destrutivos.

1. Introduction

Rails are the most important element of the track superstructure and economically hold the greatest cost among all elements of the permanent way [1-3]. As result, railway operators are constantly being pressured to increase efficiency and profitability of business. In an environment which the railroad tracks are exposed, pressured by axle loads increasing and train frequency, it has been deteriorating considerably [4-6]. In such an unfavorable operating environment, wear and defects on rails are becoming more common and faster. Special attention is placed to welded joints, regardless type of welding process. Since the weld zone is a fragile point of union between two rails and has mechanical and metallurgical characteristics worse than the base metal (parent rail) the defects in the welds act as a failure mode of rails and cause its replacement [4,7-10].

Among various methodologies of rails welding, flash butt process would be the most efficient, due to its mechanization when compared to the field welding process (thermite welding), also called aluminothermic welding [9-12]. Thus, the quality parameters of flash butt welding tend to be higher than the other processes [7,8,13]. In addition, flash butt welding is applied

Received: 09 Jan., 2020. Accepted: 29 July, 2020.
E-mail: brassenra@yahoo.com.br (BSO)

in greater quantity than thermite welding [3,8], and for that reason, it is noticed that flash butt presents a representative number of fractures after installed on track [3,8]. Figure 1 shows a rail surface defect in a flash butt welding after it is installed on track and must withstand the stresses from the wheel-rail contact. This defect, known as squat, consists of continuous material loss on the top surface of the rail, increasing the impact load coefficient and potential fracture of the flash butt weld, the defect is suitable once this paper presents the rails are installed on the track with relevant initial residual stress values, which can accelerate the formation of squats defect [2,9,14].

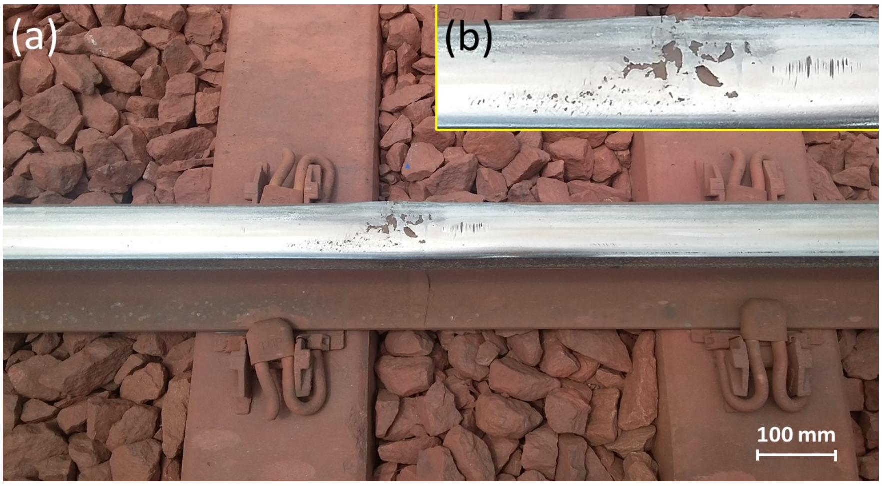

Figure 1. (a) Rail joint defect on flash butt welded rail after installation on track and load applied to welded joint; (b) detail of rail welding surface defect.

After removing external forces applied on the material (or sample) the remaining stresses are characterized as residual stresses [15]. These forces can be tensile, or compressive. Tensile forces are conducive to shear and can lead the material to rupture, compressive forces tend to compress a body applying pressure [16,17]. These stresses are generally imputed into the material after it passes through thermal and / or mechanical processes [16-18]. Some examples of processes that may add residual stresses in rails are: casting, rolling, forging, welding, machining, bending, pressing, straightening and heat treatments.

This study aims to make an analysis of the residual stresses presented in the region, welded by flash butt technology, between two rails with 370 HB surface hardness. An experimental study was carried out to measure residual stresses in the welded region. Nowadays, the methodologies applied to measure residual stress in rails require destructive (rail web sawing), semi destructive (blind hole test), laboratory techniques (strain gauges), being necessary to remove samples off the track and sending to laboratories. This paper differentiation is to pursue a non-destructive test technology [16,17,19] for the residual stress measurement, so technology could be applied on field (on track), thus the selected technology was the X-ray diffraction.

2. Experimental Procedures

2.1. Materials

The tests were performed using pearlitic rails [20-22] AREMA 136RE standard, with a 10-inch rail head radius. The rails used to carry out the tests are manufactured by JFE Steel and shows, in average, surface hardness of 370 HB, the hardness of the material decreases as the measurement is made along the inner layers of the rail [20,21,23]. However, this paper focused on the measurement of subsurface residual stresses. The rail manufacturing process is through the reduction of iron ore in blast furnaces, then the material passes through the steelworks, lamination, heat treatment and straightening [21,24].

The rails, analyzed, are acquired in bars of 24 meters in length and welded in larger bars, called continuous welded rail – CWR [25]. In the railroad where the study was conducted the length of the CWR is customized into ranges from 96 to 360 meters long [2]. The chemical composition [20], as well as the main mechanical characteristics, of the rails used in the tests are presented on Table 1.

Table 1. Chemical composition and mechanical properties (Yield Stress – YS, Tensile Stress – TS and Elongation) of the analyzed rail sample.

Chemical composition (%)							Mechanical properties		
C	Si	Mn	P	S	Cr	V	YS	TS	Elongation
0.79	0.17	0.99	0.03	0.02	0.16	0.03	853 MPa	1240 MPa	12.80%

2.2. Welding procedures

The beginning of the rail flash butt welding is the storage of short bars (24 meters) in the material yard. When the short bars are directed to the welding plant the first activity consists of grinding the ends of the rails, so all impurities, paints marks, rust or any material that may become an internal defect in the weld shall be removed. Welding occurs through the stationary machine Schlatter GAAS 80, where the welding process is flash butt. The welding parameters for pre-heating were current 69 kA (phase shift), total of 12 pulses, 3.7 seconds each pulse. About final flashing 17 mm of displacement and 1.5mm/sec of end velocity. Finally upset force adjusted to 580 kN and 4 seconds of holding time.

After welding, there is a considerable hardness decrease on rail head, once it is thermally treated, at HAZ (heat affected zone) due to the thermal input caused by the welding. HAZ on rail flash butt welding presents lengths from 35 to 40 mm, depending on carbon content and thermal input, thus based on this parameters HAZ was defined as 20mm to each side of weld – 40 mm in total [1,5,26]. These properties are reasonably recovered through the controlled cooling process of the HAZ (called air quenching). Then, the finishing rail surface grinding is performed in order to remove the excess of material that has not been cut by the welding machine, so an abrasive grinding is applied. Finally, the stress inputted during the whole process can create distortions on rail and welds and it must be re-aligned, this straightening occurs through the hydraulic pressure, again inclusion of mechanical stresses can be imputed [8,14,27].

2.3. Residual stress measurement

The equipment used for measuring residual stress was the XStress 3000 G3, manufactured by Stresstech, with waves length 2.291Å, voltage 25 kV and current was 6 mA [28]. The measurement points were cleaned by electro-erosion, using commercial reagent added to 10 ml of H_2SO_4, per litre, in this cleaning and the minimum reaction time was 10 minutes. The propagation area of residual stress measurement was 7.0 mm^2 on each measured point, due to the X-ray beam (3 mm in diameter). The accuracy of residual stress measurements was ± 20 MPa [15,16,28].

Measurements were performed on three axes, as shown in Figure 2, where the X-axis measurement presents residual stress values transverse to the rail (σx), Y-axis measurement presents residual stress values vertical to the rail (σy) and Z-axis measurement presents residual stress values longitudinal to the rail (σz) [1,5,15].

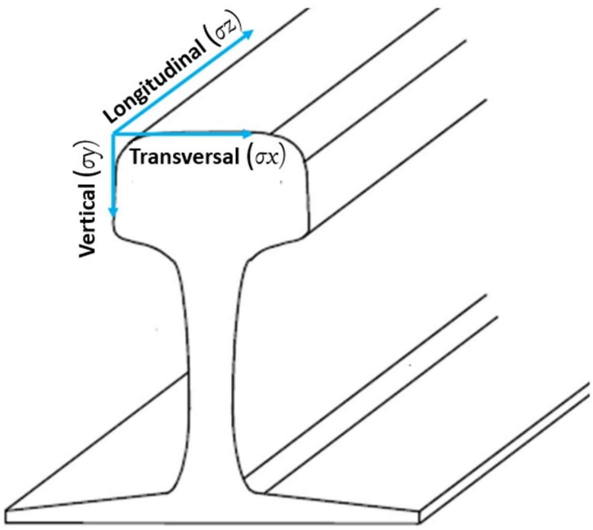

Figure 2. Residual stress measurement: three axis of the rail.

Residual stress measurements were performed in 4 different steps, as shown in Figure 3, these steps are presented:

- Step 1: Measuring residual stresses at center line of top of the rail (known as rail head). Measurements of transversal (X axis) and longitudinal (Z axis) residual stresses were performed, as shown in the Figure 4a;
- Step 2: Measuring residual stresses at rail head top edge (known as rail corner). Measurements of transversal (X axis) and longitudinal (Z axis) residual stresses were performed, Figure 4b;
- Step 3: Measuring residual stresses at lateral of the rail head, Figure 4c. Vertical (Y axis) residual stress measurements were performed. It was not possible to measure residual stress in the longitudinal (Z axis) direction due to interference between the rail base and the base of the analyzer goniometer base;

- Step 4: Measuring residual stresses at central part of the rail (known as rail web), Figure 4d. Vertical (Y axis) residual stress measurements were performed. There was the same interference between the rail base and the goniometer base, and due to it was not possible to measure longitudinal (Z axis) residual stress.

The total sample length is 200 mm, with 100 mm for each side of the weld line, located at the center of the sample. Residual stress measurements were made in HAZ region, with 20 mm for each side of the weld [1,26] and with 5 mm spacing between the measurements points. Measurements were also made in the region of the base metal (parent rail), 50 mm after the HAZ and spaced 10 mm between the measuring points. The stress values between measurement points were defined by interpolating the two closest points, in order to construct the residual stress graph. Finally, there is a 30 mm overlap at the ends of the sample where no measurements were performed, since the focus of this paper is the area affected by the weld.

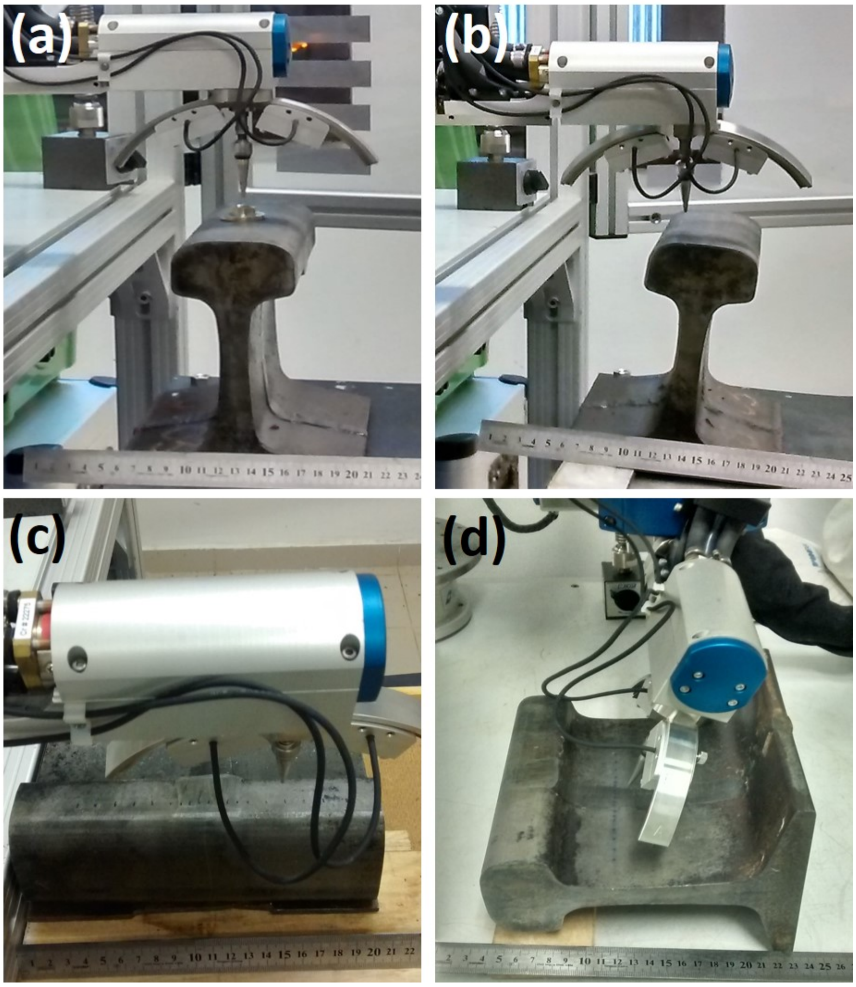

Figure 3. Positioning of rail for residual stress measurements by X-ray diffraction: (a) step 1: residual stress measurement at center line of top of the rail; (b) step 2: residual stress measurement at corner of top of the rail; (c) step 3: residual stress measurement at rail head lateral; (d) step 4: residual stress measurement at rail web.

3. Results and Discussion

3.1. Step 1: residual stress at central line of top of the rail

A longitudinal (Z axis) residual stress measurement was made, with X-ray diffraction on Z axis (**σ_z**). Then, a measurement of residual stresses transverse to the rail was made, with X-ray diffraction on X axis (**σ_x**). The residual stress measurements in the central line of top of the rail are shown in Figure 4a and shows the region near to the centre of the weld tensile stress was observed [1,29]. Values measured by the X-ray diffraction showed tensile values of 391 MPa. We can see an alternation in the type of stress as it moves away from the central line of the weld [13]. This alternation in stress field matches the residual stress graph format on welded rails which should be in the form of a letter "c", this residual stress graphs alternation is classified as C-Shape graph [5,12,19]. We can observe when closer to the center of the weld, the higher values of tensile stresses and, as it moves away from the region of the weld, the values of tensile stress decrease, and compressive stresses appears near to the ends of the sample.

Higher tensile residual stresses are concentrated in the central region of the sample, weld line [7], due to flash butt process provides a great thermal input. During welding, electric pulses are generated at the ends of the rail in order to heat the ends, as soon as heated rails are pressed against each other and the welding happens without need addition metal. In this process it is possible to induce thermal stresses (heating of the ends) and mechanical stresses (in the upset step and cutting material excess) [13].

We can see at HAZ region there are discontinuities in the tensile stress measurements. There are large oscillations in the values measured, this variability can be explained due to the metallurgical transformations that occur in the HAZ region. The thermal inputs can lead the base metal to a spheriodization of the perlite matrix (cementite phase degradation) [26], this transformation is the reason for residual stresses variations [5,7,8,19]. Heat inputs during the flash butt welding, in combination with the cooling rates applied after the welding, generates metallurgical transformations in welded region, thus contributing to the variability of the residual stresses in measurement [7,25,26,29,30].

Also, in Figure 4a, it is observed a displacement of the stresses field to the right side of the graph, that is, higher tensile stresses more concentrated on one side of the weld. This displacement, that appears at same sense of upset stage, once the peaks happens at same distance than the up-set (17mm) of the welding machine, thus it be explained by the technique the rails are welded. After heated, one of the rails is pushed over to the second, in the stage known as upset (i.e.: one of the rails is fixed and other is pressed against the first rail) [8]. Another possibility for this displacement in the stresses concentration may be the cutting of excess material from the welding after the upset step. When one rail is pushed against the other, there will be an excess of material that needs to be removed, it means, the excess material shall be cut by metal strips, and after the air quenching step there is a need for abrasive grinding in the welded region, generating large tensile surface stresses in this region and x-ray diffraction (as a sub superficial measurement) can be influenced by this grinding [31,32].

3.2. Step 2: residual stress at corner of top of the rail

A new measurement was made at the corner of the top of the rail. A longitudinal residual stress measurement was made, with X-ray diffraction on Z axis ($\boldsymbol{\sigma_z}$). Then, a measurement of residual stresses transverse to the rail was made, with X-ray diffraction on X axis ($\boldsymbol{\sigma_x}$).

Measurements made at corner of the top of the rail presented values lower than the first measurement (step 1), since the lateral is the external part of the rail and allows greater heat exchanging [13,32,33]. Another point differs this measurement in relation to the first one, is that higher homogeneity in the distribution of the stress along the HAZ was observed. Even so, we still visualize the eccentricity of the tensile stress field, same factor that happened during measurements in central line of top of the rail.

The same stress profile was verified again, i.e., displaced tensile stresses closer to the welded area [1]. As it moves away from this region, it can be seen the stress field changing to compressive. Once more, the C-shape profile was evident [5,12,19]. Figure 4b shows the values measured during this step. The variability of residual stresses in HAZ was also observed, just as occurred in step 1.

3.3. Steps 3 and 4: residual stress at rail head lateral and rail web

Finally, measurements were made, this time at the rail head lateral. The first measurement was made vertically (Y axis) to the rail, with X-ray diffraction on Y-axis ($\boldsymbol{\sigma_y}$). In sequence, vertical residual stresses were measured on the rail web with X-ray diffraction on Y-axis ($\boldsymbol{\sigma_y}$). Figure 4c shows measurements taken from rail head lateral and (orange line) as well as rail web (red line). The values obtained in the measurements are shown in sequence.

Again, closer to center line of the weld higher tensile residual stresses are presented, as it moves away from the weld, the stresses tend to be compressive. There is also a displacement in distribution of stresses field, more concentrated to one side of the rail, in the same way as had already been shown in previous measurements. It is also possible to visualize that the residual stresses at rail head lateral have distribution peaks, as already evidenced previously, due to the metallurgical transformations [7,25,26,29,30].

Measurements made on rail web presented better symmetry of values if compared to rail head stress values. The tensile stress levels are close to 250 MPa and the measurements performed in HAZ showed great similarity [5,7,8,19]. No displacement on residual stress curve was observed at rail web unlike what occurred in the rail head, regarding the sample was not submitted to any type of blasting. It is known that the head region suffers grinding, air cooling, heat treatment and straightening, but in rail web these processes are not applied contributing to explain the reasons of rail web region presenting more homogeneous values [1]. Zero values at rail extremities represents the unmeasured regions, once the focus of this paper is the HAZ. Important to reinforce this paper is focusing the discussions based on residual stress measurements and thermal effects of the flahs butt welding is not being discussed.

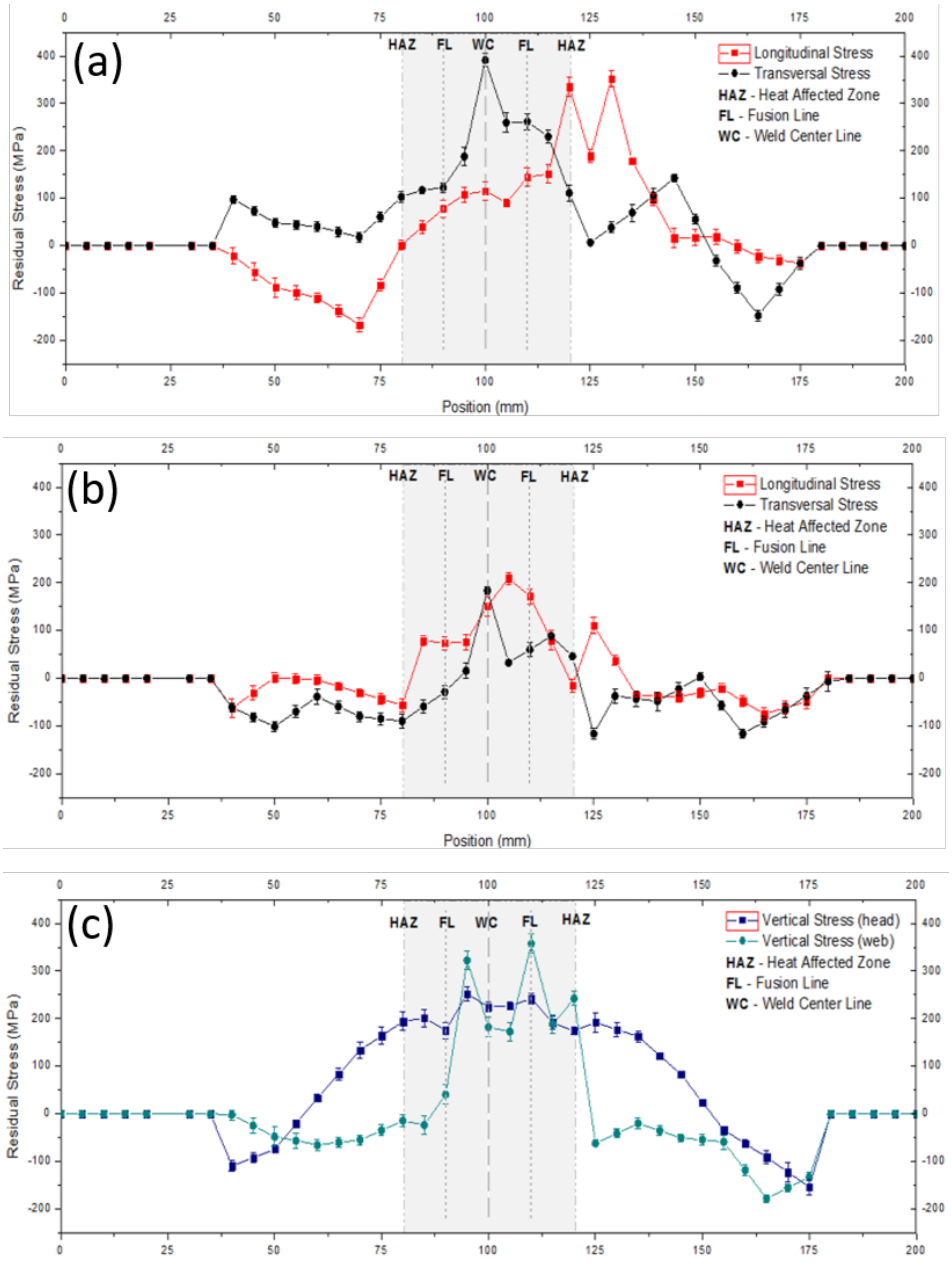

Figure 4. (a) Residual stress measurement, in MPa, at center line of top of the rail. Longitudinal Stress, σ_z (red line) and Transversal Stress σ_x (black line); (b) residual stress measurement, in MPa, at corner of top of the rail. Longitudinal Stress, σ_z (red line) and Transversal Stress σ_x (black line); (c) Vertical residual stress (σ_y) measurement, in MPa, at the rail head lateral (blue line) and rail web (green line).

3.4. Surface map of the residual stresses

Given the measurements made in the top of the rail, Figure 4a together with the measurements made in the lateral of the top of the rail, Figure 4b it can be plotted, using Autodesk and Autocad Software, a representation of the distribution of residual stresses along the entire surface of the top of the rail. This representation is made through the projection of the values presented in the referred Figures and subsequent filling the missing stresses through the gradient values that complete the gaps of stresses [16]. This representation is presented in Figure 5 showing the surface map of the top of the rail, which arises from an interpolation of all the measurements previously made in the region of top of the rail [16].

The Figure 5 represents a consolidation of Figures 4a and 4b, presented previously, and we can see the general distribution of the residual stresses at rail head. It is showed that closer to the weld line tensile stresses are found and, as it moves away from weld line, the residual stress tends to be compressive [1]. There is also a displacement in the stress distribution, which is more concentrated to one side of the rail. It is also possible to visualize the residual stresses presenting peaks in rail head and rail web. In rail head the peaks an heterogeneous and on rail web the peaks are concentrated close to flash butt welding. Rail head stress peaks are already showed in the Figures presented in this paper.

Residual stress measurements showed results from subsurface stress, since the X-ray diffraction does not have a long measuring range. Thus, the residual stresses in rails tend to be higher at the surface, since the surface hardness higher than the inner part of the rails. Thus, the X-ray diffraction technique can be considered effective, due to the measurements were consistent to other techniques and the values presented on this paper are on same magnitude of the classical papers related to rail flash butt welding technique [16,19,33].

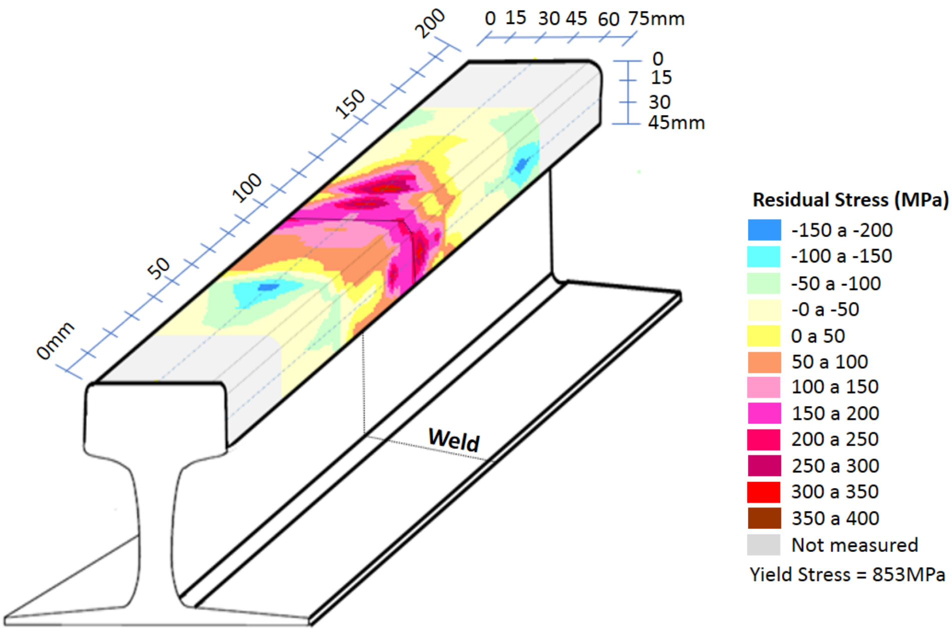

Figure 5. Residual stresses distribution on top of rail after welded by flash butt technique.

4. Conclusions

Current techniques for measuring residual stress in rails requires destructive or semi-destructive tests, which makes it unappropriated to be applied when rails are installed in track. This paper evaluated the application of a non-destructive test, in this case, X-ray diffraction, for measurement of residual stress in the flash butt welded zone on rails. The technique proved to be effective during the measurements performed and the results of the experimental procedure were consistent and innovative considering this study presents the residual stress in a complete welding process, including: pre-grinding, flash butt welding, heat treatment, finishing grinding and straightening.

It was observed higher values of residual stress are in the weld line of the top of the rail head, with tensile stresses up to 391 MPa and in the central part of the rail head lateral with tensile stresses closer to 350 MPa. It was identified that evaluated regions have residual stresses greater than the rail residual stress before weld, increasing up to 60% the residual stresses in rail head. Due to the results, the welding process contributes to the increase of the residual stresses on rails, as well as the additional steps of the welding process, such as grinding, heat treatment and straightening.

Results are promising, since the technique was efficient and, considering it is a non-destructive methodology, it can be improved for field application, something that is not currently applied. In this way, an accurate monitoring of the welds installed in track can be made introducing greater predictability of failures, reducing the track interdiction times and reducing the probability of railroad accidents.

Acknowledgements

Authors of this paper thanks to Federal University of Para, to the Process Engineering Post-Graduation Program (PPGEP), to the team of Materials and Metallic Characterization Laboratory (LCAM), to the Mechanical Engineering School, to Vale S/A company, Carajas Railway Engineering Department and everyone whom contribute to this paper.

References

[1] Saita K. Developing technologies to improve the reliability of flash butt welds. In: Proceedings of the 11th International Heavy Haul Association Conference; 2017 Sept 2-6; Cape Town. Virginia Beach: International Heavy Haul Association; 2017. p. 208-215.

[2] Vale S.A. Manual técnico de via permanente. São Luís; 2013.

[3] Xiao G, Xiao X, Guo J, Wen Z, Jin X. Track dynamic behavior at rail welds at high speeds. Lixue Xuebao. 2010;11(26):449-465. http://dx.doi.org/10.1007/s10409-009-0332-9.

[4] Gutscher D. Inovative rail welding methods. In: Proceedings of the Transportation Technology Conference; 2012 Mar 13; Pueblo, Colorado. Pueblo, CO: Transportation Technology Center; 2012. p. 4793.

[5] Tawfik D, Mutton PJ, Chiu WK. Alleviating tensile residual stress in flash butt welds by localized post-weld heat treatment. Journal of Materials Processing. 2008;196(1-3):279-291. http://dx.doi.org/10.1016/j.jmatprotec.2007.05.055.

[6] Transportation Rail Corporation. Annual report 2012-2013. New South Wales, Australia; 2012.

[7] Cai Z, Nawafune M, Ma N, Qu Y, Cao B, Murakawa H. Residual stresses in flash butt welded rail. Transactions Joining and Welding Research Institute. 2011;40(1):79-87.

[8] Mansouri H, Monshi A. Microstructure and residual stress variations in weld zone of flash butt welded railroads. Science and Technology of Welding and Joining. 2004;9(3):237-245. http://dx.doi.org/10.1179/136217104225012201.

[9] Mutton PJ, Alvarez EF. Failure modes in aluminothermic rail welds under high axle load conditions. Engineering Failure Analysis. 2004;11(10):151-166. http://dx.doi.org/10.1016/j.engfailanal.2003.05.003.

[10] Salehi S, Khodabakhshi B, Mutton P, Paradowska A. Aluminotermic welding of rails: improved qualification and performance under heavy haul conditions. In: Proceedings of the 2014 Conference on Rail Excellence; 2014 May; Adelaide, Australia. Washington: The National Academies of Sciences, Engineering, and Medicine; 2014.

[11] Railtech. Aluminotermic welding procedures: technical catalogue. Paris; 2005.

[12] Schleinzer G, Fischer FD. Residual stress formation during the roller straightening of railway rails. International Journal of Mechanical Sciences. 2001;43(10):2281-2295. http://dx.doi.org/10.1016/S0020-7403(01)00041-8.

[13] Federal Railroad Association. Structure and properties of thermite welds in premium rails. Washington: US Department of Transportation; 1985. p. 124.

[14] British Standard. EN 14578:2007: railways applications – track – flash butt welding on rails. London; 2007.

[15] Universidade Federal do Pará – UFPA. Laboratório de Caracterização de Materiais Metálicos – LCAM. Relatório de medição de tensões residuais em trilhos ferroviários. Belém: LCAM; 2017.

[16] Costa ES, Assunção PDC, Santos EBF, Feio LG, Bittencourt MSQ, Braga EM. Residual stresses in cold wire gas metal arc welding. Science and Technology of Welding and Joining. 2017;10(17):7. http://dx.doi.org/10.1080/13621718.2017.1306014.

[17] Kelleher J, Prime MB, Buttle D, Mummery PM, Webster PJ, Shackleton J, et al. The measurement of residual stress in railway rails by diffraction and other methods. Journal of Neutron Research. 2003;11(4):187-193. http://dx.doi.org/10.1080/10238160410001726602.

[18] Talamini B, Gordon J, Perlman AB. Finite element estimation of the residual stress in roller straightened rail. In: Proceedings of the 2004 ASME International Mechanical Engineering Congress; 2004; Anahein, US. New York: ASME; 2004. p. 9.

[19] Tawfik D, Kirstein O, Mutton PJ, Chiu WK. Verification of residual stress in flash butt welded rails using neutron diffraction. Physica B, Condensed Matter. 2006;385-386:894-896. http://dx.doi.org/10.1016/j.physb.2006.05.242.

[20] American Railway Engineering and Maintenance-of-Way Association. Chapter 4: rails. Detroit: AREMA; 2016.

[21] Bramfitt BA. A metallurgical perspective of the role of rail steel in the growth of America. Warrendale: AIST; 2011.

[22] Carrol RI. Surface metallurgy and rolling contact fatigue of rail [thesis]. Sheffield: Sheffield University; 2005.

[23] British Standard. EN 13674:2007: railways applications – track – rail – part 1: vignole railway rails 46kg/m and above. London; 2007.

[24] National Physical Laboratory. NPL materials centre report. Teddington: NPL; 2001.

[25] Hurlebaus S. Determintation of longitudinal stress in rails. Texas: Transportation Research Board; 2011.

[26] Nishikawa LP, Goldenstein H. Divorced eutectoide on heat affected zone of welded pearlitic rails. Materials Journal. 2019;71(2):815-823.

[27] Fuji M, Nakanowatari H, Nariai K. Rail flash butt welding technology. JFE GIHO. 2004;34:109-113.

[28] Stresstech. X-Stress 3000 G2/G2R: X ray stress analyzer. Technical catalogue. Mumbai; 2018.

[29] Kuchuk-Yatsenko SI, Velikoivanenko EA, Rozynka GF, Shvets YV, Didkovsky AVI. Investigation of residual stress in welded joints of rail produced by flash butt welding. EO Paton Welding Journal. 2004;9:32-35.

[30] Withers PJ. Residual stress and its role in failure. Reports on Progress in Physics. 2007;70(12):2211-2264. http://dx.doi.org/10.1088/0034-4885/70/12/R04.

[31] Kandil FA, Lord JD, Fry AT, Grant PV. A review of residual stress measurement methods: a guide to technique selection. Teddington: National Physical Laboratory; 2001. p. 45.

[32] Zerbst U, Lundén R, Edel K-O, Smith RA. Introduction to the damage tolerance behavior of railway rails: a review. Engineering Fracture Mechanics. 2009;76(74):2563-2601. http://dx.doi.org/10.1016/j.engfracmech.2009.09.003.

[33] Ma N, Cai Z, Huang H, Deng D, Murakawa H, Pan J. Investigation of welding residual stress in flash-butt joint of U71Mn rail steel by numerical simulation and experiment. Materials & Design. 2015;88:1296-1309. http://dx.doi.org/10.1016/j.matdes.2015.08.124.